NAVY DEPARTMENT
BUREAU OF ORDNANCE
WASHINGTON 25, D. C.

Vice Admiral G. F. Hussey, Jr., USN
Chief of the Bureau of Ordnance

Captain K. H. Noble, USN
Assistant Chief of Bureau for Research

Captain S. H. Crittenden, Jr., USN
Ammunition and Explosives

Dr. Stephen Brunauer,
High Explosives and Amphibious Munitions

Research Group in Theoretical Physics

NAVORD Report 7-47

INTERFEROMETRIC STUDY OF SUPERSONIC PHENOMENA

Part III

Boundary Layer and Shock Wave Interactions Observed Along Probes and Wires in Supersonic Air Streams

J. Winckler

Palmer Physical Laboratory
Princeton University
Princeton, New Jersey

19 February 1947

NAVY DEPARTMENT
BUREAU OF ORDNANCE
WASHINGTON 25, D. C.

19 February 1947

NAVORD REPORT 7-47

INTERFEROMETRIC STUDY OF SUPERSONIC PHENOMENA, Part III: Boundary Layer and Shock Wave Interactions Observed Along Probes and Wires in Supersonic Air Streams.

1. NAVORD Report 7-47 presents data on the interferometric studies of supersonic phenomena and is the third of a series of reports on this subject published for the use of agencies conducting research on supersonic flow.

2. This report presents preliminary data and therefore does not constitute a final comprehensive study. Additional information and criticism by other agencies for incorporation in future reports is requested.

3. The findings herein represent the interpretations of the author and are not necessarily the views of the Bureau of Ordnance. The work has been done under contract NOrd 9240 at the Palmer Physical Laboratory, Princeton University. The technical liaison officer of the Bureau of Ordnance is Dr. F. J. Weyl.

4. This report does not supersede any existing publication.

G. F. HUSSEY, JR.
Vice Admiral, U. S. Navy
Chief of the Bureau of Ordnance

Captain, U. S. Navy
Asst. Director, Research
and Development Division
By direction

ABSTRACT

In earlier reports of this series it was shown how quantitative values of density, pressure, temperature, velocity and Mach number in supersonic gas streams could be obtained optically by the use of an interferometer. The Mach number M may be obtained independently by making shadow photographs of the head wave of a narrow probe placed in the stream. Probe and interferometer Mach number values were in good agreement in a homogeneous stream from a Laval nozzle, but in complete disagreement in an inhomogeneous expanding air jet in the region where standing shock waves occur. This discrepancy has been traced to the influence of the standing shocks on the air flowing at low velocity in the boundary layer along the probe. The shock pressure may cause a separation of the stream from the probe, and a configuration of normal and oblique shocks arises as a result at the region of separation.

Further experiments made in a strictly one-dimensional stream show an analagous separation of flow when a normal standing shock wave intercepts the boundary layer. The theory of separation is discussed in the light of some earlier work of Prandtl and Stodola.

Part III

Boundary Layer and Shock Wave Interactions Observed Along Probes and Wires in Supersonic Air Streams

I. INTRODUCTION

In Part I of this series of reports 1/ an interferometric analysis was made of a typical supersonic air jet. This report includes the details of the methods of applying the Mach interferometer to an axially symmetric flow pattern, and the density distribution in such an air jet from a circular orifice was determined. As set forth in section VI - 7 of that report, an effort was made to correlate Mach number values calculated from the density with those measured directly by probes, with the result that large discrepancies were observed in the region of the air jet where shocks were present. Good agreement is observed, however, in streams without shocks, for example, parts of the jet near the orifice and in the uniform stream from a Laval nozzle. 2/ A brief explanation for this effect in terms of shock wave-boundary layer interactions was given in Section VI-7 of Part I. The present report gives a detailed explanation of the effects observed with probes in jets, as well as some further experiments carried out with axial wires in a circular homogeneous stream from a Laval nozzle.

1/ INTERFEROMETRIC STUDY OF SUPERSONIC PHENOMENA Part I. "A Supersonic Air Jet at 60 lb/in.^{2} Tank Pressure." NAVORD Report 69-46

2/ Comparison of Interferometer and probe Mach numbers in the homogeneous stream from a Laval nozzle is described in detail in NAVORD report 93-46 "INTERFEROMETRIC STUDY OF SUPERSONIC PHENOMENA PART II. "The Gas Flow Around Various Objects in a Free Homogeneous Supersonic Air Stream."

II. EXPERIMENTAL RESULTS

Figure 1 is a spark shadowgram of an air jet, from a smoothly converging round nozzle of 10 mm. orifice diameter, with tank overpressure of 60 lbs./in.^{2}. The standing shock waves are produced by the expansion and contractions of the jet as it proceeds from the orifice.

By means of interferometer technique as described previously (Part I) the density distribution in this jet was obtained optically with good accuracy. The use of various hydrodynamical equations, together with the initial tank conditions, enables one to obtain the pressure, velocity, temperature and Mach number everywhere in the jet. In particular, the Mach number can be obtained from the relation

$$M(\rho) = \left\{ \frac{2}{\gamma - 1} \left[\left(\frac{\rho_0}{\rho} \right)^{\gamma - 1} - 1 \right] \right\}^{\frac{1}{2}} \qquad (1)$$

where ρ_0 is the tank density, and ρ is the density corresponding to the Mach Number M. This equation contains the adiabatic relation, and is therefore valid only in isentropic regions of flow, which in the air jets in question means the region bounded by the standing shocks and the boundary layer where the jet mixes with the room air. Mach number values downstream from the standing shocks may be calculated from the analagous relation

$$M(\rho) = \left\{ \frac{2}{\gamma - 1} \left[\frac{T_0}{T_2} \left(\frac{\rho_2}{\rho} \right)^{\gamma - 1} - 1 \right] \right\}^{\frac{1}{2}} \qquad (2)$$

where T_0 is the tank temperature, T_2 and ρ_2 are the temperature and density of gas immediately on the downstream side of the shock, which may be obtained from the known shock strength and angle by applying the Rankine - Hugoniot relations. The Mach number in turbulent regions can not be calculated in a simple way from the density. These equations show that the flow is supersonic everywhere except in a core extending downstream from the normal shock wave.

If the flow is supersonic, i.e., $M = \frac{u}{a} > 1$,

the Mach number may also be obtained by making shadowgrams of the headwave of a fine probe pointed into the stream, and measuring the angle α of the headwave to the stream direction. The stream direction coincides with the headwave bisector if the cone is narrow, as shown by Kopal 3/. The Mach number is then given by $M(\alpha) = \frac{1}{\sin \alpha}$.

3/ Private Communication from Z. Kopal, Massachusetts Institute of Technology. For example, the shock-cone yaw ratio = .01 for a 5 degree cone and .1 for a 10 degree cone at Mach number 1.70.

Best Available Copy

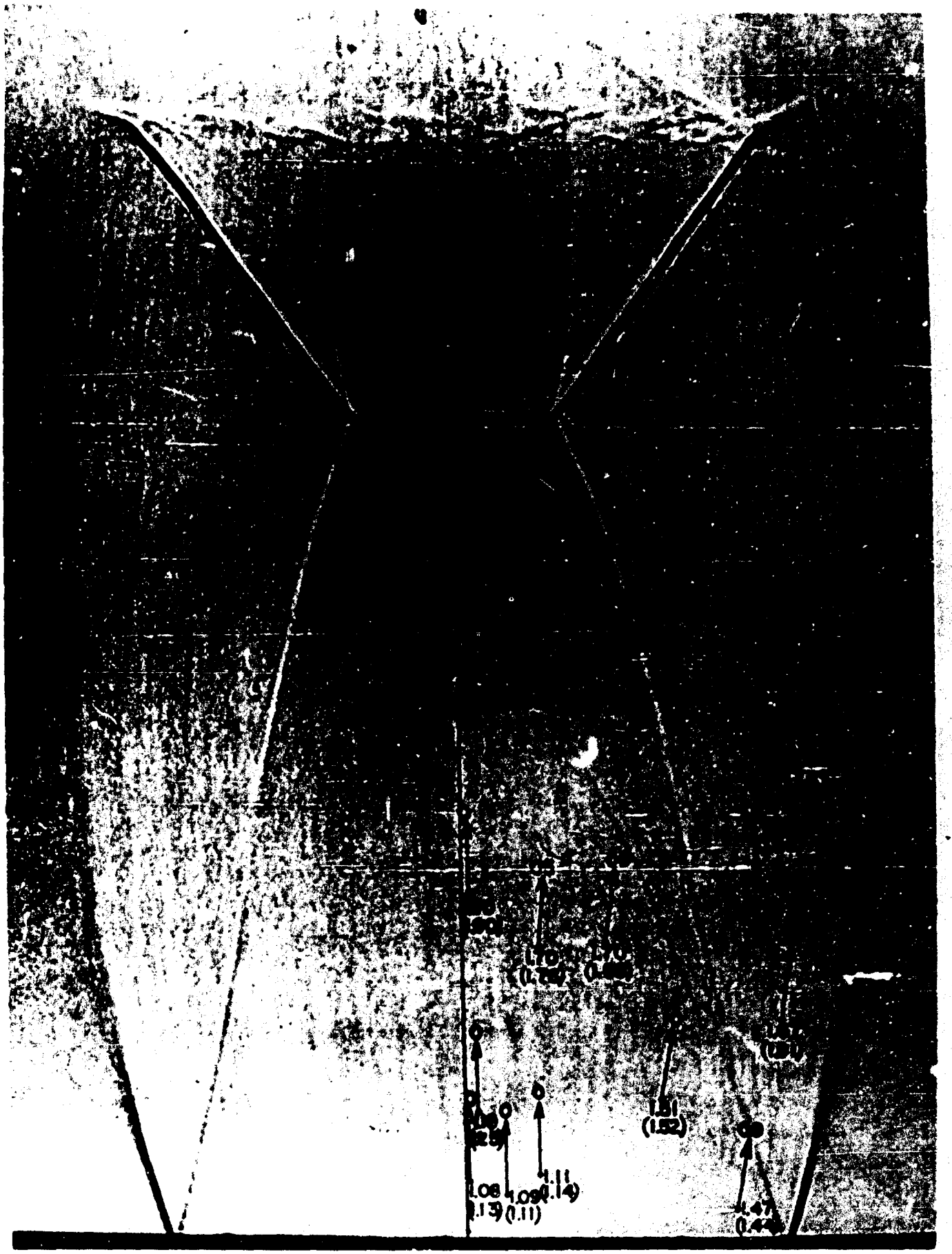

Figure 1. Shadowgram of a supersonic air jet from a converging round orifice (Tank pressure, 60 lbs/in.^{2}). The arrows give the air velocity as measured by a probe (degrees from vertical at arrow head, Mach number at tail). The Mach numbers in parenthesis are obtained from the interferometer. For explanation of values in ▭ see text page 4.

Both methods of determining M have been applied to an air jet from the 10 mm converging nozzle at $P_o = 60$ lbs/in.^{2} overpressure. Figures 2 and 3 are typical shadowgrams showing the appearance of the probe headwave near the orifice and near the shock region respectively. In addition photos were made with the probe in many other locations. In Figure 1 the resultant M values are tabulated, the arrow pointing in the stream direction and having its tail at the place of measurement; M (α) is given at each point and M (ρ) (from Equation (1) or in a few cases (2)), just below in parenthesis. The agreement is satisfactory at the orifice region, but the M (α) values are generally different than the M (ρ) values in the jet boundary, as would be expected as equations (1) and (2) do not apply in turbulent regions. Probe values are probably correct in this region. Large deviations occur, however, in the region upstream from the normal shock wave, which is an isentropic region. M (ρ) is here 200 - 300% larger than M (α). (These M (α) values are enclosed in boxes).

A qualitative comparison of shadowgrams such as Figures 2 and 3 showed that on the basis of the width of the dark band in the probe headwave shadow a much stronger shock wave formed about the probe point in Figure 3 than in Figure 2, appearing as if the probe had drawn down the normal shock with it as it was inserted. The shape of the jet, of course, is completely changed on the downstream side of the probe when it is inserted. The oblique shocks in Figure 2, for example, appear closer to the orifice than normally.

Six interferograms of the 60 lb. jet were made with the probe in positions similar to Figures (2) and (3) and at other intermediate points between the orifice and the normal shock. Figures 4 and 5 illustrate two cases, with the probe near the normal shock and near the orifice respectively. Three or four cross sections were measured on each interferogram at the approximate positions with respect to the probe indicated by the cross lines. The jet without probe had been completely measured previously.

The initial conditions were approximately the same in all cases, namely, 60-lb/in.^{2}. tank overpressure and room temperature.

The sections near the orifice gave no detectable difference with and without probe, from which we conclude that the head wave appearing in the shadowgrams of Figure 2 represents a density step $\Delta\rho$ too small to be detected by the interferometric analysis at the existing radius.

The results near the shock region with the probe point at $z = 11.30$ mm. are shown in Figure 6, resulting from an analysis of the interferogram of Figure 4.

The densities up to the position of the probe shock wave agree with and without probe as closely as could be expected for different photographs. But a strong shock is present in the cross sections with the probe, inclined at $\alpha = 54^\circ$ to the stream .

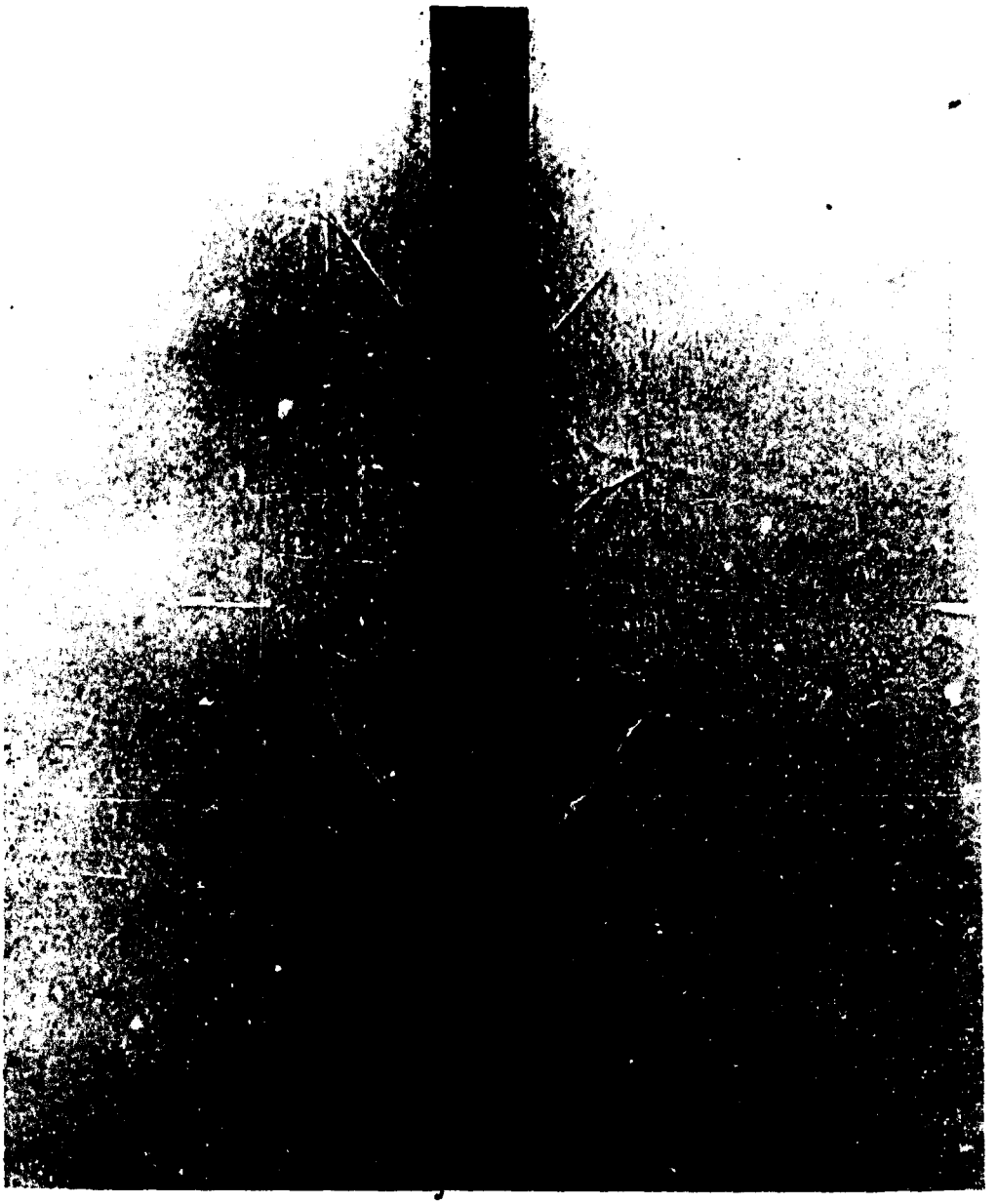

Figure 2

Probe measurement of Mach number near the orifice (Spark shadowgram)

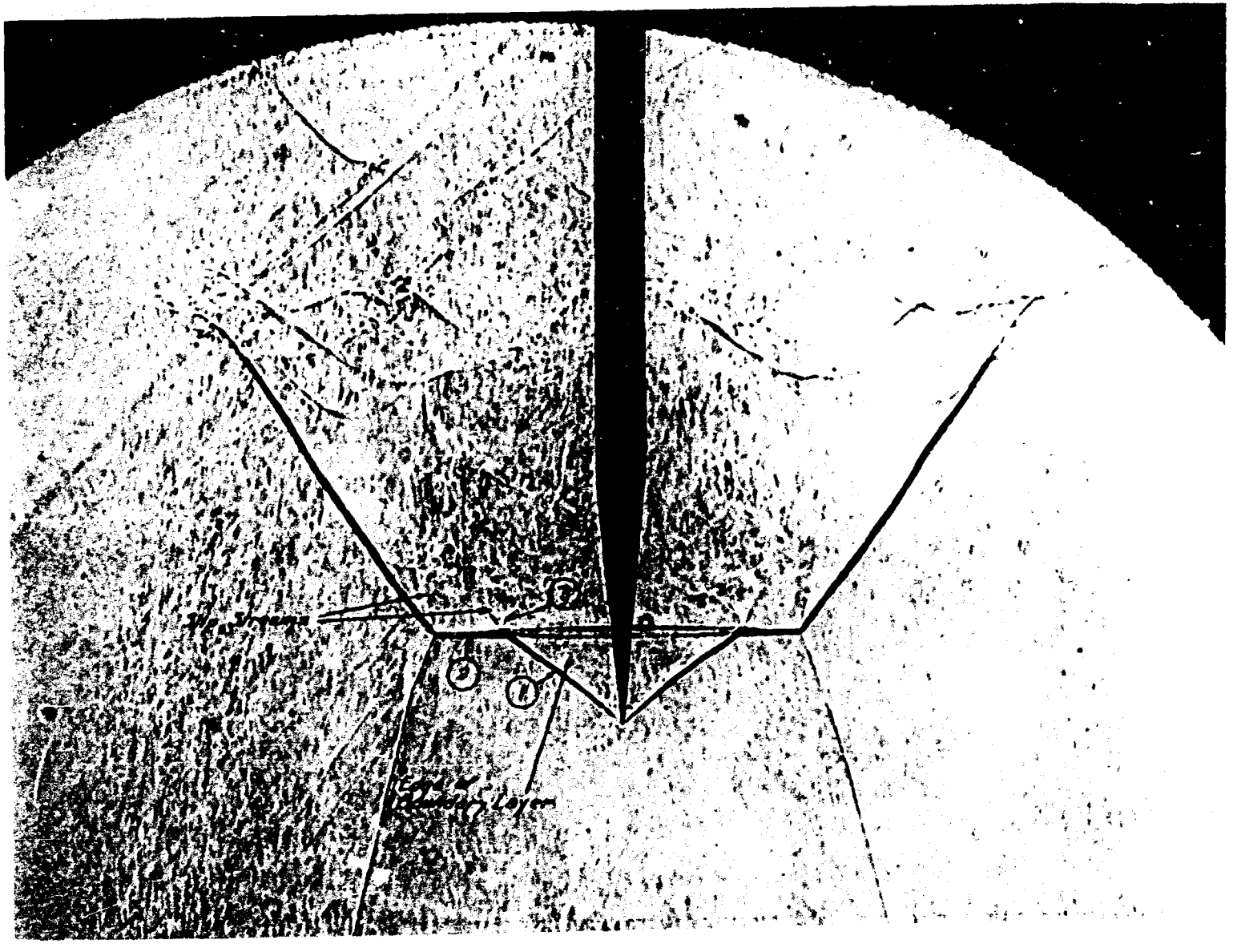

Figure 3

Probe for measuring Mach No. near the shock region (Spark shadowgram). The shocks have been numbered in accordance with Figure 9. (See text page 14)

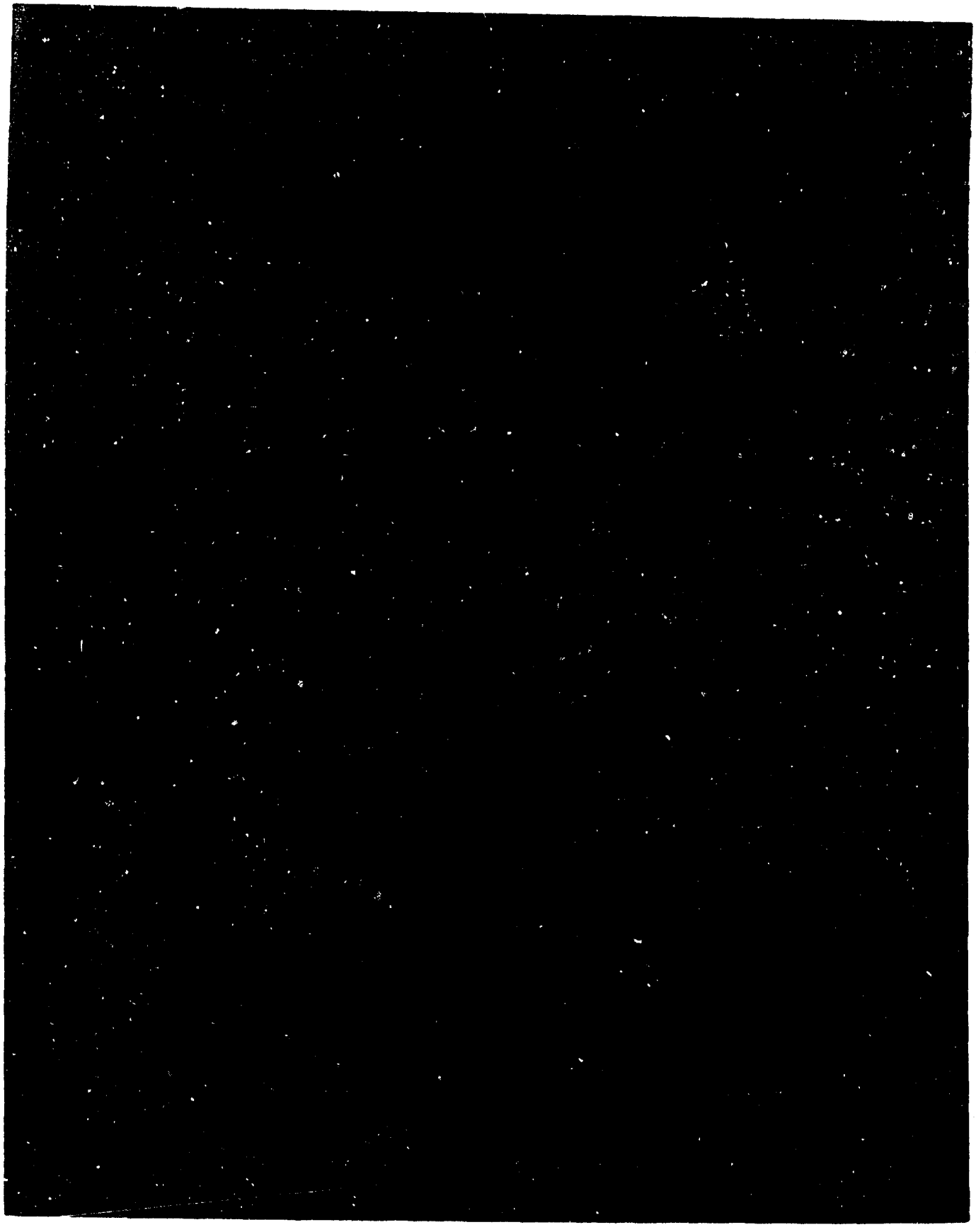

Figure 4

Interferogram of air jet with probe near the shock region. Cross sections at A-A, B-B, C-C, and D-D were evaluated. (see Figure 6)

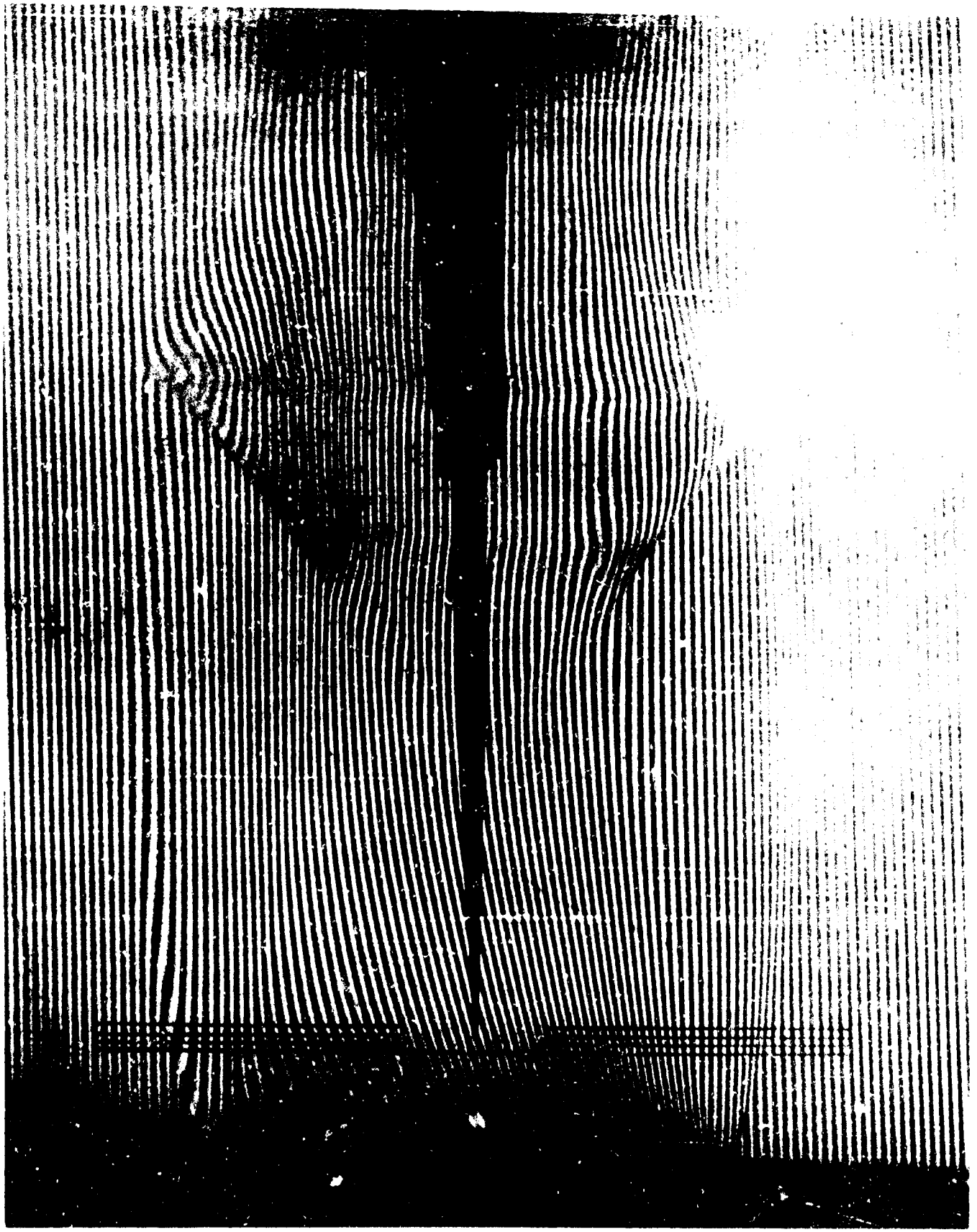

Figure 5

Interferogram with probe near the orifice. The indicated cross sections [illegible]. The probe head shock in this case is too weak to be detected interferometrically.

Table I. Calculated and observed values of ρ_2/ρ_1 for the shocks about the probe as evaluated from six interferograms.

Position of Probe Point z (mm)	Position of Cross Section z (mm)	M total*	M_n	ρ_2/ρ_1 Eq. (11)	ρ_2/ρ_1 Observed
11.30	12.10	3.03	2.44	3.3	3.4
	11.82	2.97	2.41	3.2	3.3
	11.58	2.95	2.39	3.2	3.0
9.43	10.61	2.71	2.05	2.7	2 8
	9.86	2.60	1.93	2.6	2.4
8.04	9.92	2.63	1.79	2.3	2.3
	8.42	2.38	1.50	1.9	1.8
6.67	8.61	2.43	1.43	1.7	1.9
	7.61	2.23	1.28	1.5	1.6
5.78	No shock detectable on interferogram				
2.48					

*M total was obtained from the density in the stream directly before the shock front from equation (1).

The equation

$$\frac{\rho_2}{\rho_1} = \frac{\frac{1}{2}(\gamma+1)}{\frac{1}{M_n^2} + \frac{1}{2}(\gamma-1)} \qquad (3)$$

which gives the shock strength as a function of the Mach number component M_n normal to the shock front was applied to the shocks about the probe evaluated from the six interferograms, and gives good agreement with the measured values as shown in Table I.

A continual decrease in shock strength occurs as the probe is brought nearer the orifice, until at about z = 6 mm, the shock is too weak to show on the interferograms. It is just at this region that the values given in Figure 1 come into agreement, within the experimental error.

Thus the strength and angle of the shock formed at the probe is consistent with the high Mach number in the stream as calculated from the density. The large discrepancies in Figure 1 arise from using the simple equation

$$M = \frac{1}{\sin \alpha}$$

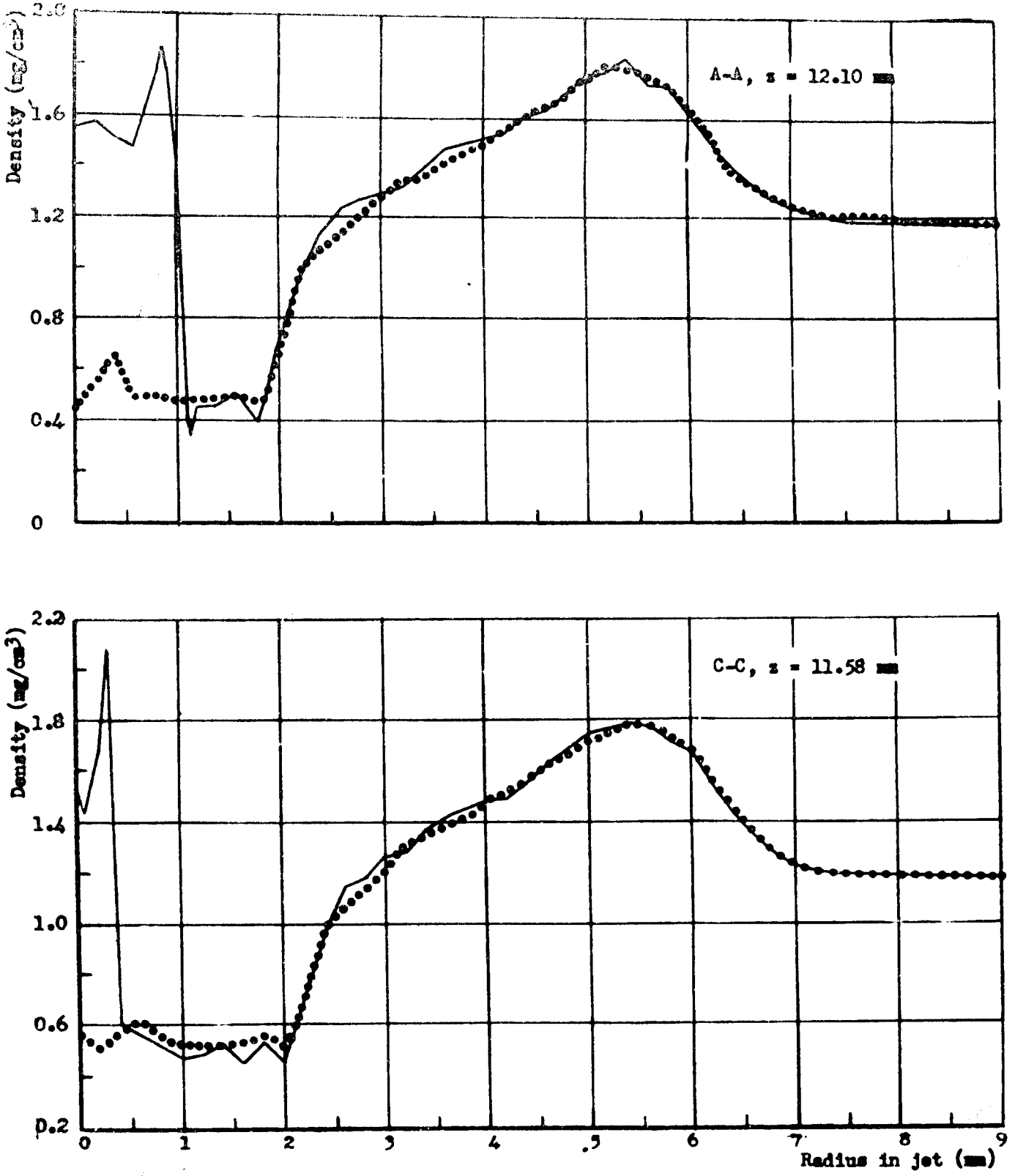

Figure 6 - Density cross sections with probe; ———, jet + probe; ....., jet without probe.

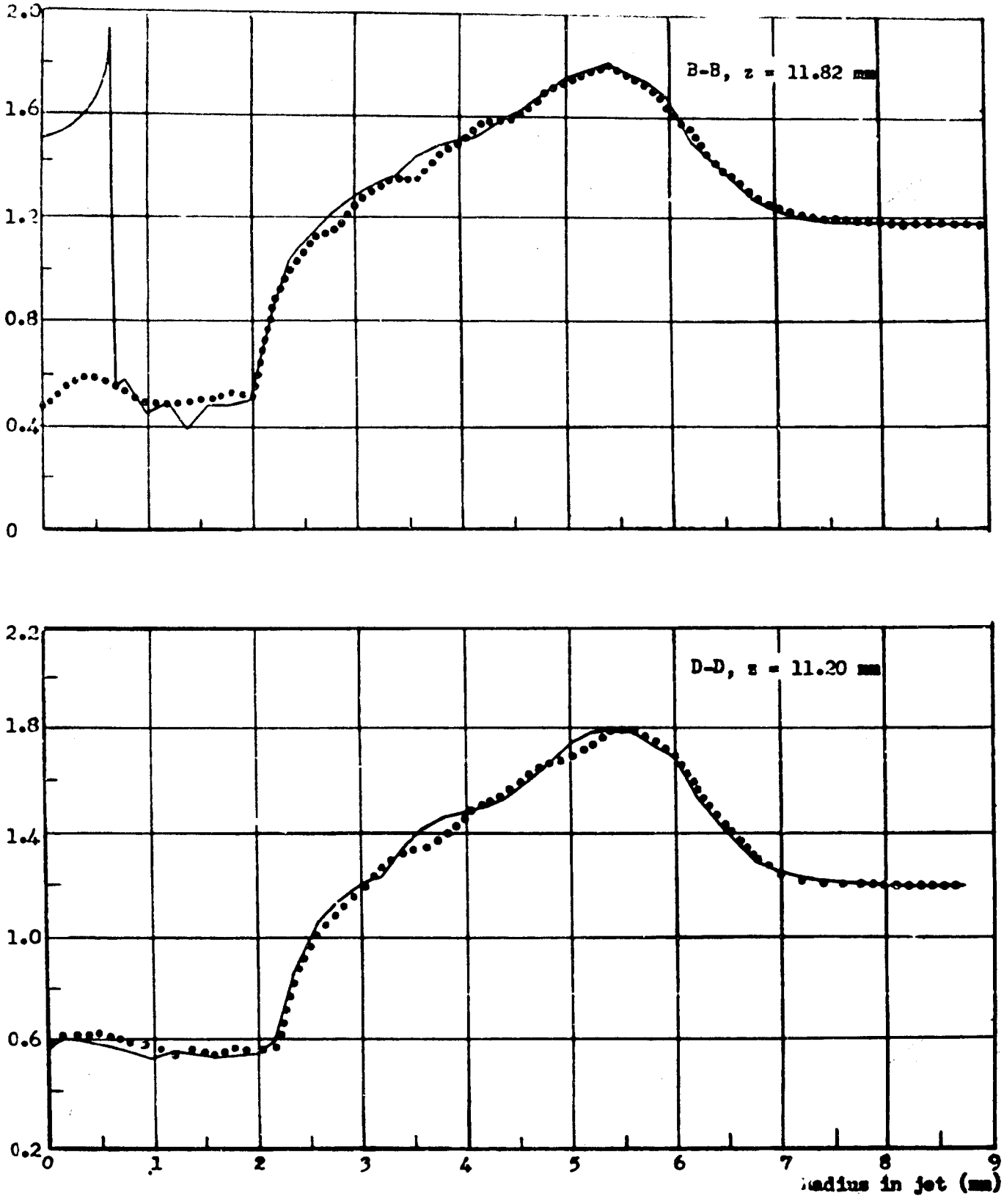

Figure 6 cont'd - Density cross sections with probe; ——, jet + probe; ·····; jet without probe.

which gives the true Mach number only if the probe head wave is very weak, and travels approximately with the sound velocity a. For strong shocks the velocity is higher, and 1/sin(merely gives the ratio

$$\frac{M}{M_n} = \frac{M \cdot a}{M_n \cdot a}$$

of the total Mach number to the component normal to the shock front, as the shock velocity is equal and opposite to the component of the gas velocity normal to the shock front and the total gas velocity before the shock is M.a.

The problem is then to explain the formation of the strong shock appearing as if it were the probe headwave. The well-established theory of the supersonic flow about conical objects (e.g., the theory of Taylor and Maccoll 4/) predicts that the headwave of a very narrow cone should be a very weak shock and should be inclined at the Mach angle α. It is known that a second solution of the flow equations exists, representing the other possible shock having the proper strength and inclination to divert the flow by the necessary amount to pass the cone. But the possibility that the strong shock represented a "second solution" for the cone problem was discarded in the light of the following explanation:

A close examination of the shadowgrams with the probe brought through the normal shock revealed the presence of a "dead water" region, conical in shape, beginning at the point of the probe and extending downstream from it. The stream appeared to be diverted outward, and measurements actually showed that the probe headwave angle corresponded roughly to that which would be obtained if the dead water were considered to act on the stream like a solid cone. Following a conversation with Dr. Hans Liepmann of the Guggenheim Aeronautical Laboratory the possible influence of boundary layers was considered.

It is a well-known fact in fluid dynamics that a transition layer exists at the boundary of a fluid stream in which the velocity of flow decreases from the free stream velocity down to zero at the wall. This boundary layer may be laminar or turbulent depending on the Reynold's number and various conditions of stability. 5/ At any rate, the velocity becomes subsonic in the boundary layer of a supersonic stream, providing an opportunity for signals to be propagated upstream along the wall.

It is also known that the stream may separate from the wall, resulting in a large thickening of the boundary layer which extends out into the body of the fluid if the pressure increases in the direction of the flow.

4/ Taylor and Maccoll, Proc. Roy. Soc. 139, 278 and 298 (1933) Maccoll, Proc. Roy. Soc. 159, 459 (1937). See also Part II of this series of reports for comparison between experiments and Taylor and Maccoll's theory.

5/ See "Modern Developments in Fluid Dynamics" ed. by Goldstein for a discussion of boundary layer phenomena. Also various NACA publications.

Prandtl 6/ has explained this phenomenon for an incompressible fluid, assuming that the stream pressure persists unchanged through the boundary layer. Fluid in the layer is pulled along by the free stream, but retarded by the wall and by the adverse pressure gradiant. In certain cases it may actually be brought to rest, or made to flow in the reverse direction, resulting in a back eddy, and a diversion of the main stream. (See Prandtl, loc. cit., Fig. 2, page 4, or Goldstein, Fig. 22, page 57). The point of separation may be calculated, provided $\frac{\partial P}{\partial x}$ is given everywhere, by experiment or otherwise, and occurs where $\frac{\partial V}{\partial y}$ becomes greater than zero.

It should be noted that while in subsonic flow a stream may be diverted into itself or compressed in a continuous manner, at supersonic speeds such a compression occurs either entirely discontinuously by means of a shock wave, or partly discontinuously and partly continuously. Thus if the boundary layer separates in a supersonic stream, an oblique shock wave must occur to provide the necessary diversion of the stream. This is shown in Figure 7, which is analagous to Prandtl's drawing, but for the supersonic case.

FIGURE 7
STREAM SEPARATION ACCOMPANIED
BY A SHOCK WAVE.

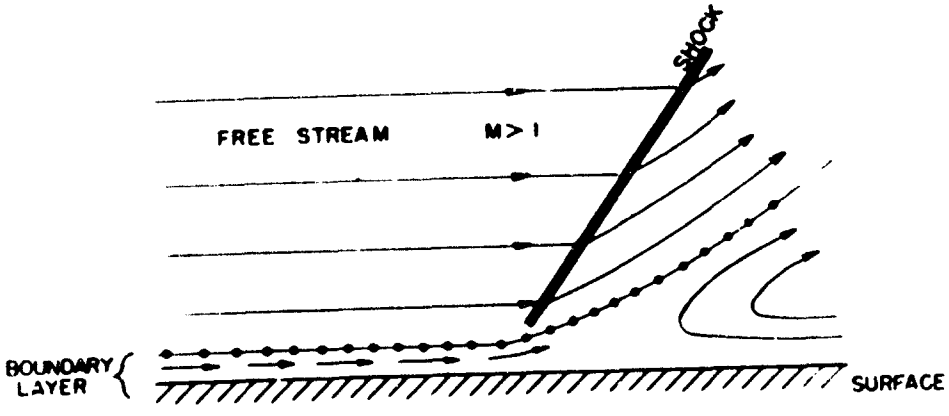

6/ "Vier Abhandlungen zur Hydrodynamik und Aerodynamic" L. Prandtl and A. Betz. Gottingen 1927

A situation of this kind may arise if a boundary layer is present at a normal shock. In Figure 8 a stream of Mach number M_1 and pressure P_1, accompanied by a boundary layer in

FIGURE 8
NORMAL SHOCK WAVE
AND
BOUNDARY LAYER

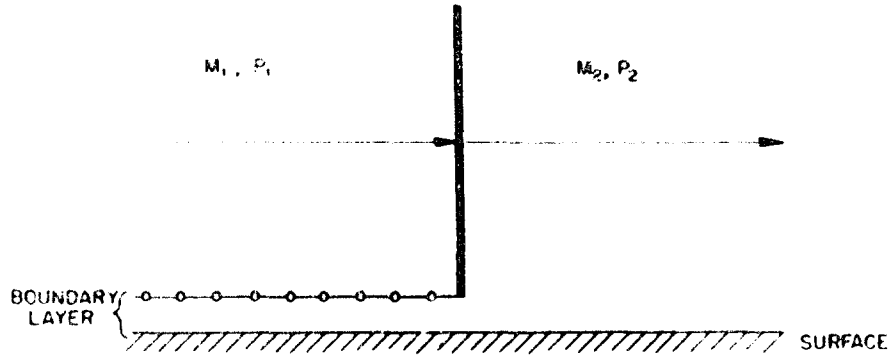

which the pressure is also P_1 encounters a normal shock, across which the pressure rises to P_2. The situation as shown in Figure 8 will certainly be unstable if the shock has a finite strength, i.e., if P_2 is appreciably greater than P_1. Flow in the boundary may be retarded or stopped by the pressure increase, and the stream will be diverted. This explanation is certainly over-simplified as the normal shock can in no case extend down into the boundary layer where the flow is subsonic. The pressure distribution around the foot of the shock is rather obscure, but it is certain that a pressure increase does occur, and a stable situation of the type shown in Figure 9 exists.

FIGURE 9
INTERACTION OF A NORMAL SHOCK WAVE WITH THE BOUNDARY LAYER

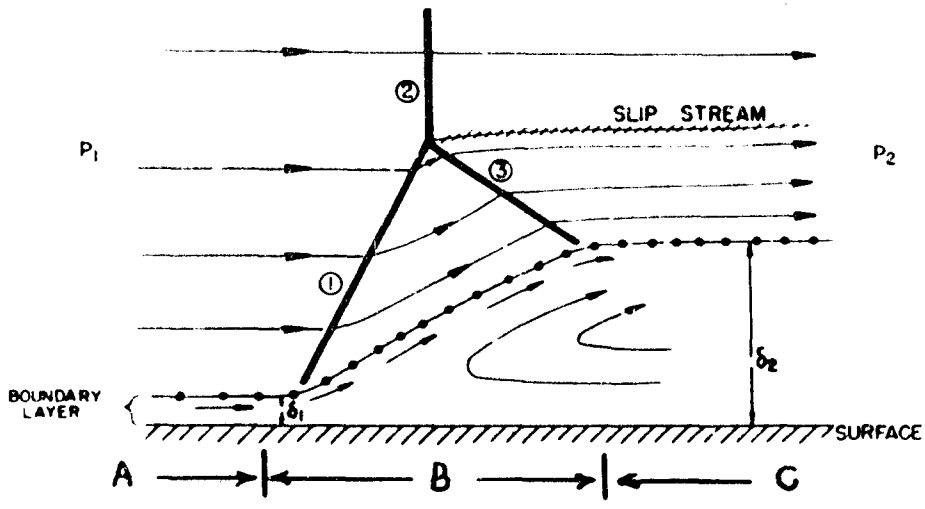

The overall result is to transfer the stream and boundary from the region A at pressure P_1 to the region C at pressure P_2, the vortex sheet meanwhile retreating from the wall from δ_1 to δ_2 . The initial divergence of the stream is accomplished by shock ①. If the normal shock ② is to remain, a third shock ③ is required to return the stream to its initial direction. Strangely enough, a three shock interaction thus exists. The usual slipstream arises at the shock intersection, which is present in addition to the boundary layer in region C But since the pressures on the two sides of a slipstream, or throughout a boundary layer are equal, region C must be a region of uniform pressure, which is determined uniquely by the Mach number and pressure at A by the usual Rankine-Hugoniot formula

$$\frac{P_2}{P_1} = \frac{2\gamma M_1^2 - \gamma + 1}{\gamma + 1} . \qquad (4)$$

That a situation analagous to Figure 9 actually does exist in the vicinity of the probe is shown by Figure 3. The various shocks and slipstreams have been numbered to correspond to Figure 9. One can observe the stream separation at the probe point, and the strong shock wave through which the divergence (compression) occurs, arising from the probe point.

The slipstream from the three-shock intersection is more plainly visible than the boundary layer edge as it is a much larger discontinuity.

The phenomenon of stream separation through shock waves which explains the anomalies observed with probes in jets actually occurs quite generally in supersonic gas flow. Stodola 7/ describes separation phenomena in steam nozzles, including an effect with a probe similar to the present case. His photographs, although not very clear, also show a three-shock-separation from the wall of a nozzle, and this is further confirmed by pressure measurements. The peculiar impact pressure curves obtained by surveying a diameter of the stream nozzle near the separation point (Stodola, Figure 54) are probably the result of traversing successively a supersonic, subsonic, and again a supersonic region (for example, a vertical section just downstream of shock 2, Figure 9). The pitot pressure obtained by bringing the tube near the downstream side of a normal standing shock should be the same as the free stream pitot pressure, since the tube generates its own normal shock wave in the free stream. But the loss of impact head is less through a series of oblique shocks plus the pitot shock than through the pitot shock alone, and therefore the pitot pressure rises in the region downstream of shock 2, (Figure 9).

For subsonic flow the stream may leave the wall of a diffusor (expanding channel), as the pressure in the direction of flow increases in this case. (See Goldstein, Plate 5, page 58). In the supersonic flow of a gas, an expanding channel implies a pressure decrease, and therefore no tendency for the flow to separate. The equation

$$\frac{dA}{A} = \frac{dP}{P} \cdot \frac{1}{\gamma}\left(\frac{1}{M^2} - 1\right) \qquad (5)$$

shows that for $M < 1$, dP is in the same direction as dA, but in the opposite direction for $M > 1$. In certain cases, however, such as an expanding nozzle emptying into the atmosphere, the gas may find itself expanded below atmospheric pressure, and the adverse pressure gradient up to atmospheric pressure separates the stream from the nozzle wall.

Figure 10 shows three phases of such a separation. These photographs are spark shadowgrams of air emerging from a tank through a Laval nozzle of circular cross section consisting of a straight portion, an expanding portion, and a final straight portion of 1.2" diameter. The end of the nozzle is the black shadow at the bottom of the picture. If the tank pressure is adjusted to about 4.5 atmospheres, the stream emerges homogeneous and parallel, with a Mach number of 1.70, and at very nearly atmospheric pressure. 8/ This nozzle actually constitutes a small open wind tunnel. (Experiments with such an open wind tunnel were reported in Part II of this series)

7/ Stodola, "Steam and Gas Turbines". Vol. I, McGraw-Hill 1927, Section 33, Page 88-94.

8/ The relation between tank pressure P_0 and jet pressure P is given by

$$P = P_0\left[1 + \frac{\gamma-1}{2} M^2\right]^{\frac{\gamma}{\gamma-1}} \qquad (6)$$

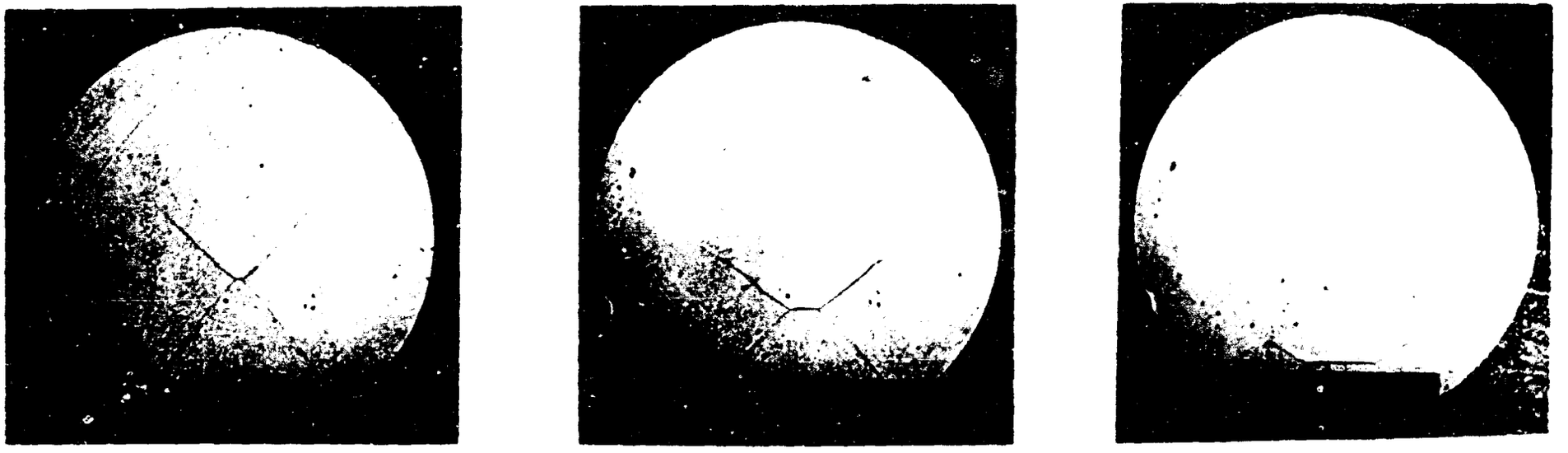

A
Jet Press =
0.7 Atmos.

B
Jet Press =
0.6 Atmos.

C
Jet Press =
0.4 Atmos.

Figure 10.

Separation of Flow from Nozzle in a Supersonic Stream
Discharging at Less than Atmospheric Pressure

If the tank pressure is decreased to 3.4 atmos., Figure 10-A results. The jet emerges at less than atmospheric pressure (0.7 atmos.), but still practically fills the inner bore of the tube. The stream is pressed inward by the atmosphere immediately upon leaving the orifice, and the change in direction is accomplished by an "incident" compression shock. This shock is of course cone shaped, but only portions tangential to the parallel light beam are revealed. The stream is again made parallel to its original direction by the "reflected" shock and continues at supersonic speed. The flat normal shock in the center is typical of the three-shock formation which occurs whenever the strength and angle of the "incident" shock can not allow a simple "reflection" involving only two shocks, and is a sort of stationary Mach effect. A slipstream (very weak and not visible on the reproduction) exists between subsonic air which passed the normal shock, and the stream outside this which has crossed the two oblique shocks and proceeds at higher velocity.

In Figure 10-B the jet emerges at 0.6 atmos. from a tank at 2.7 atmos. and has separated from the inner wall of the tube. The "incident" shock increases in strength and angle, with an accompanying change in the Mach reflection. Figure 10-C is a further stage of the phenomena, with the jet and tank pressures 0.4 atmos. and 2.0 atmos. respectively. The normal shock remains unchanged in strength as the Mach number is constant, but increases in width from A to C. If the jets of Figure 10 are divided by a line down the axis, the similarity of either part with Figure 9 is immediately apparent, and we are probably dealing with an analagous phenomenon. The configuration shown in Figure 10 has been studied in detail interferometrically and the values of shock strength, angles, etc. compared with the three-shock theory. The results will be given in a future report.

In Figures 11 and 12 an axial wire has been mounted in the nozzle previously shown in Figure 10, and the boundary layer formed along the wire then interacts with the normal shock in the manner set forth in Figure 9. The various shocks in Figures 11 and 12 have been labeled in accordance with Figure 9. In Figure 11, $M_1 = 1.70$, $P_1 = .48$ atmos. and $P_2 = 1.53$ atmos. and in Figure 12, $M_1 = 1.70$, $P_1 = .55$ atmos., and $P_2 = 1.7$ atmos., calculated from tank pressure and Mach number using equation (4) and (5). It should be recalled that this, as well as all other shadowgrams shown in this report are projections of an axially symmetric figure, as the jet is circular. This accounts for the fact that shock ② appears continuous across the wire, although in reality it has a "hole" in the middle, and the projection of the outer sections gives the appearance of a continuous shock.

The boundary layer after separation appears violently turbulent, and its edge is much less distinct than the slipstream from the shock intersection. It also appears that the greatly thickened boundary layer is soon lost by diffusion at points downstream from the normal shock.

The shock and slipstream angles have been measured in Figures 3, 11 and 12, as well as the number of other similar cases of separation, and the results compared with shock wave theory. Assuming that the stream is diverted past the dead water region like the flow about a solid cone, the angle of shock ① should be given by Taylor and Maccoll's theory

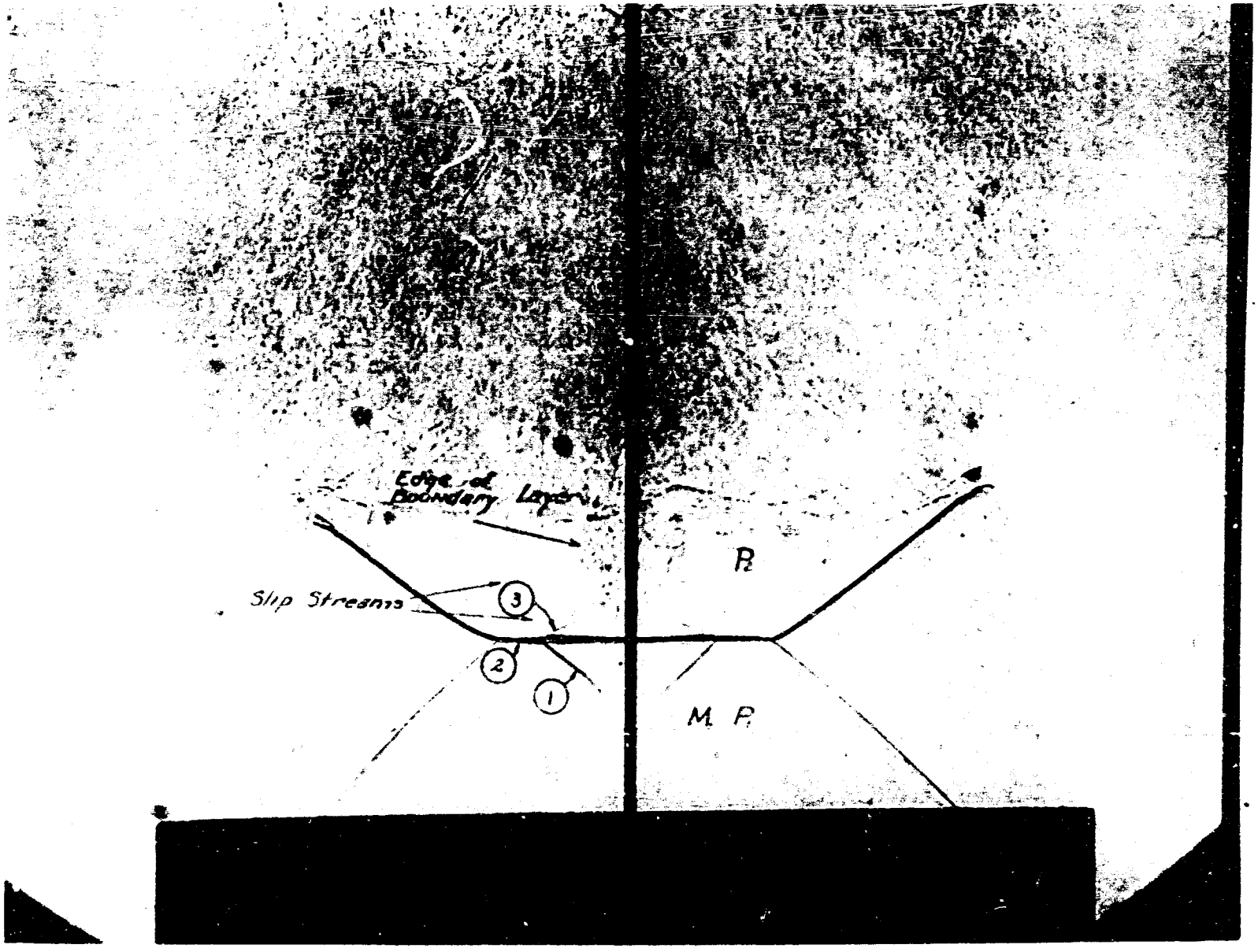

Figure 11

Homogeneous jet, (M = 1.7) with an axial wire to show effect of wire boundary layer on the normal shock. Numbered in accordance with Figure 9.

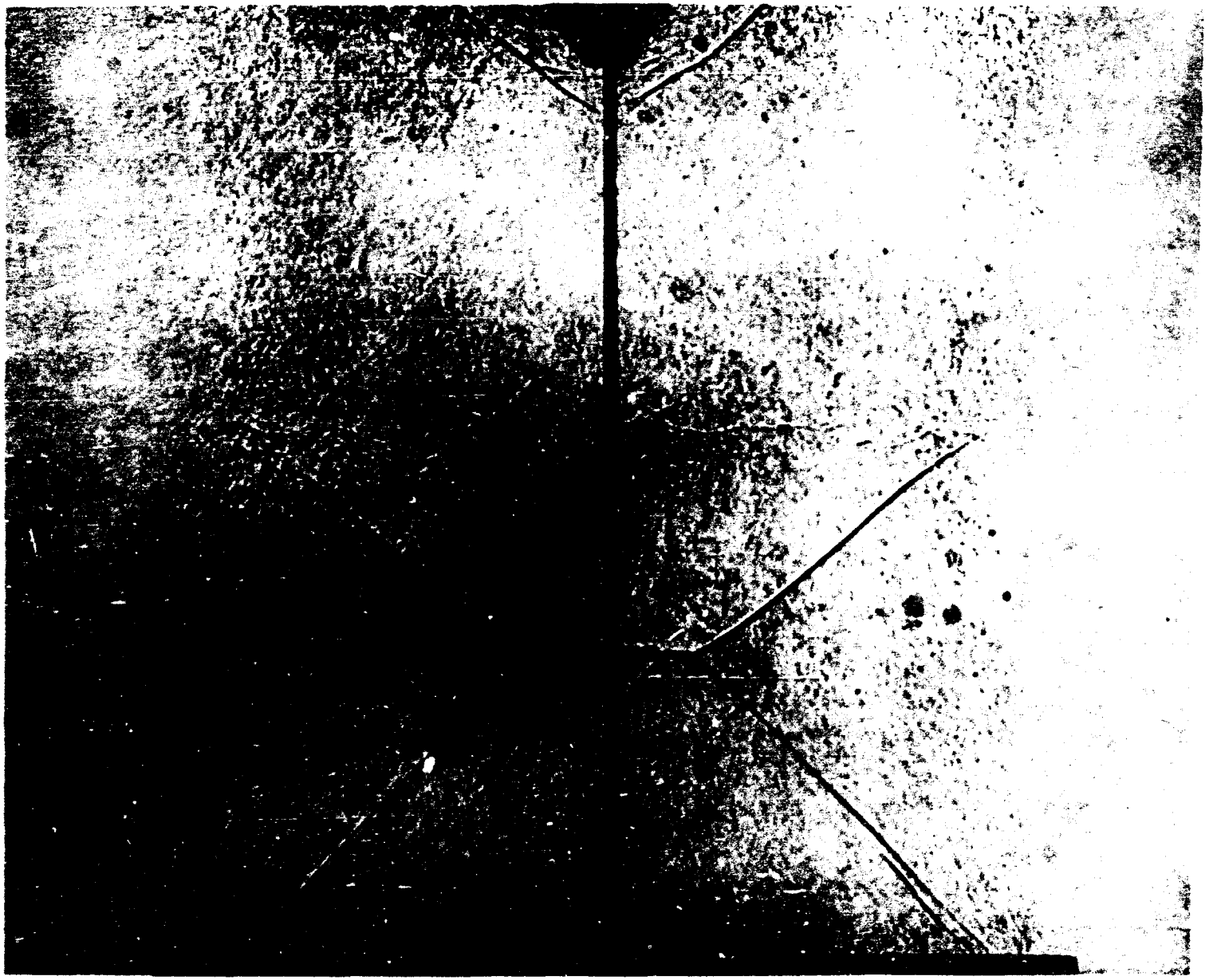

Figure 12

Same as Figure 11, but with higher tank pressure

(reference 4) in terms of the semi-angle α of the separated boundary of the dead water region. The experimental results follow:

A. Expanding air jet, similar to Figure 3, with probe.

	Mach No.	Measured Shock Angle	Theoretical Shock Angle
2° probe	1.91	24.9°	11°
	2.03	19.9	16
	2.07	21.5	16
	2.30	24.9	26
	2.51	31.8	31
	2.95	44.4	40
5.2° probe	2.14	16.3	15
	2.26	18.3	19
	2.40	27.7	24
	2.68	38.2	33
12° probe	2.35	26.1	25
	2.51	30.8	27
	2.57	35.1	30
	2.71	40.2	35

B. Homogeneous stream, Laval nozzle, with axial wire. (like Figs. 11 and 12)

	2.2	40.5	41°
	2.15	39.9	42.5
	2.04	42.2	44
	2.04	42.5	43
	1.90	41.7	42
Fig. 12	1.70	42.1	43
Fig. 11	1.70	47.9	46.5

These measurements, although rather rough, nevertheless seem to show that the interpretation of the separation phenomenon is correct. Why the separation shocks develop wider in Figure 11 than Figure 12 is not clear, as the normal shock should be originally the same in both cases.

More careful experiments should be made, to determine at which shock strength and Mach number separation sets in. The best way to study this would seem to be in an axially symmetric three-dimensional flow. In rectangular cross sectioned wind tunnels with parallel glass walls the flow tends to separate from the glass as well as from the other two surfaces when a normal shock is present, thus introducing an unknown variation in the direction of the light beam.